SSRG International Journal of Electrical and Electronics Engineering
ISSN: 2348-8379/ https://doi.org/10.14445/23488379/IJEEE-V11I4P106

Volume 11 Issue 4, 45-54, April 2024
© 2024 Seventh Sense Research Group®

Original Article

Design and Simulation of HEMT Millimeter Wave Power Amplifier for 5G Applications

Aswini Kumar Gadige[1], Paramesha[2]

[1,2]ECE Department, School of Engineering, Central University of Karnataka, Karnataka, India.

[1]Corresponding Author : aswinigadige@gmail.com

Received: 05 February 2024 Revised: 05 March 2024 Accepted: 04 April 2024 Published: 30 April 2024

Abstract - *In terms of S parameters, rollet stability factor, stability measurement, and input/output impedance, 20 High Electron Mobility Microwave Transistors (HEMT) operating at millimeter wave frequency (30 GHz) are compared in this paper. Subsequently, a comparison of the performance of basic class E PA designed with these 20 HEMTs with respect to the number of parameters, including input and output reflection, forward and reverse transmission, power added efficiency, drain efficiency, gain, stability factor, and stability measurement, was conducted. The HEMT transistor, JS8911AS, is found to be a suitable device for designing the high gain millimeter wave power amplifier circuit for the 5G transmitter communication system at 30 GHz based on the comparison analysis. The proposed stacked power amplifier and two-way Doherty power amplifier are designed with a new self-biased parallel RLC power control circuit that addresses the problems of excess power dissipation and drain gate parasitic capacitance. The output power, gain, power added efficiency, and drain efficiency of the suggested Doherty power amplifier operating at 30 GHz were found to be 28.45 dBm, 21.47 dB, 79.34%, and 80%, respectively. Keysight ADS Simulation Tool is used for all Schematics and Simulations.*

Keywords - *RF electronics, Analog electronics, Semiconductor devices, Power amplifier, 5G.*

1. Introduction

The next-generation technology that supports 5G's high data rate connectivity is millimeter wave communication. Power amplifiers are essential in this communication system because they increase the radiation from the antenna at the transmitter end. The main objective for circuit designers is to select an appropriate transistor for the high-frequency power amplifier they are developing. In general, microwave transistors are capable of functioning at microwave frequencies. These transistors operate as small signal amplifiers up to 6 GHz and power amplifiers up to 4 GHz [1].

Compound semiconductor materials such as GaAs, AlGaAs, and GaN are used to fabricate the most microwave transistors. At high frequencies and in high-power applications, these materials outperform ordinary silicon due to their hetero junction and increased electron mobility. The HEMT transistor's two-dimensional electron gas, or 2DEG, theory aids in controlling the device's conductivity and enhancing electron mobility.

High-speed applications, power amplifiers, oscillators, small signal amplifiers, and mixers working at millimeter wave frequency can all be designed using HEMTs because of their low noise performance. Therefore, the optimum devices for designing the millimeter wave power amplifier for 5G communications are the HEMT/Microwave transistors. Later, CS-CG cascoding [2] of FETs was introduced to raise the operating frequency of microwave transistors. This lowers the Miller effect by maintaining the common source FET as the input stage and the common gate FET as the output stage. Three distinct stacking techniques [3] are shown in order to achieve the watt-level output power. These techniques help to lower the parasitics present at the intermediate nodes of the CS-CG cascode and also enhance the breakdown voltage of FETs, which raises the supply voltage and increases the output power.

The traditional inductor stacked power amplifier with two biasing voltages and an output that is collected from a common gate stage is shown in Figure 1. However, huge DC power dissipation takes place due to separate gate biasing voltages for multiple stacked FETs, and the high output impedance of the common gate stage makes the designing of impedance matching circuit difficult to achieve the low output impedance and distortion less signal at load.

Usually, high-to-low impedance matching can result in signal reflections and loss of power transfer efficiency, leading to reduced overall system performance. This problem has not yet been focused on in the previous literature. In this work, a comparative analysis of 20 high electron mobility

This is an open access article under the CC BY-NC-ND license (http://creativecommons.org/licenses/by-nc-nd/4.0/)

transistors with different performance criteria is discussed. Later, these twenty HEMT transistors are utilized to model simple Class E power amplifiers, which provide 100% theoretical efficiency and consume less power [4]. To find the best HEMT at 30 GHz, the performance of these power amplifiers is compared. Lastly, a self-bias parallel RLC power control circuit is used in the construction of the suggested stacked and Doherty power amplifier with the best HEMT.

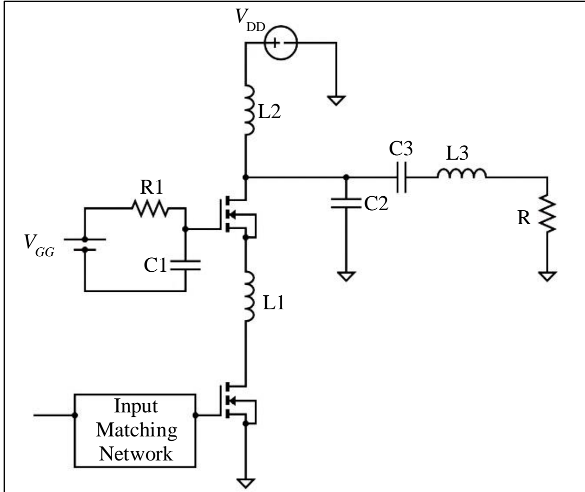

Fig. 1 Conventional stacked power amplifier

2. Class E Power Amplifier

Figure 2 shows the simple circuit of the basic Class E Power Amplifier. RFin is the radio frequency input signal, and in the case of the 5G transmitter, it is the digital modulated signal that controls the ON/OFF state of HEMT. V_{DD} and V_{GG} are drain and source biasing voltage which helps to maintain the proper operating region for faithful amplification. If the HEMT is in the cutoff region, then C, and C2 Charge through V_{DD} and in the saturation region, capacitors start discharging through HEMT to ground.

A half-wave rectified signal can be observed at the drain of HEMT, and this signal shapes into a complete sinusoidal signal at the load (R) after crossing the High Q Resonant series LC Circuit, as shown in Figure 3. Here, Ids1 and Ids2 are currents flowing through the circuit in the ON and OFF states of FET, respectively. The values of passive devices are taken based on Nathan O. Sokal, WA1HQC Equations [5]. The choice of L2, C, C2, and R values depends on the frequency of operation, biasing voltages, Output Power required, and Q Value. Class E Power Amplifier is high efficient tuned switching amplifier used for a broad range of applications in the MF, HF, and VHF bands. Multistage Cascode/Cascade, stacking, Wilkinson power divider, and combiner structure, Doherty concepts help to improve the gain, Drain Efficiency (DE), output power, and Power Added Efficiency (PAE) of Class E PA. Novel concepts like predistortion, negative feedback help to improve the linearity and stability respectively.

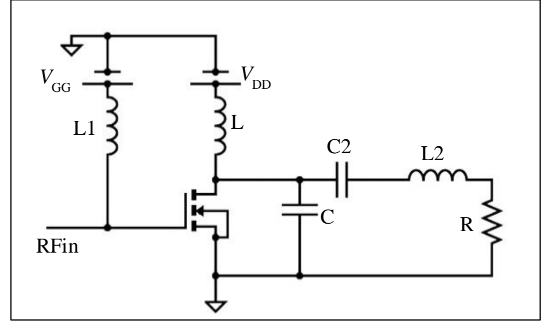

Fig. 2 Basic class E power amplifier

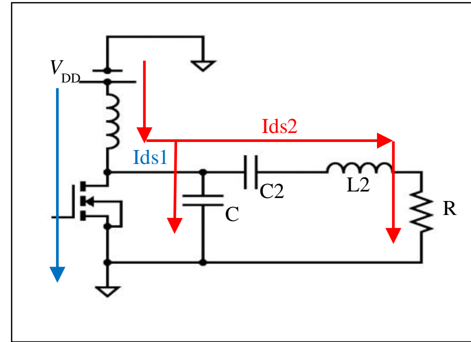

Fig. 3 Class E PA simplified drain resonant circuit

3. HEMT Comparative Analysis

High-frequency operating transistors are necessary to meet the needs of high-speed applications, including the 5G communication system. Elemental semiconductor devices exhibit parasitic elements at high frequencies, which lowers overall performance. As a result, compound semiconductor devices can help high-frequency circuits operate more effectively due to their hetero junction, large energy band gaps, and 2 DEG. Table 1 shows the absolute maximum values for the drain voltage (VDS), gate voltage (VGS), drain current (ID), power dissipation (PD), operating frequency (F), and gain of twenty High Electron Mobility Transistors.

JS8901AS, JS8902AS, JS8905AS, JS8910AS, and JS8911AS are the low-noise HEMTs manufactured by Toshiba America Electronic Components ranging the gate length from 0.1 µm to 1.3 µm. NE32400 (Ultra Low Noise Pseudomorphic HJFET), NE33200 (Super Low Noise HJ FET), NE32484A and NE32684A (Ultra Low Noise Pseudomorphic HJFET) are the HEMTs manufactured by California Eastern Laboratories.

MGFC4416C, MGF4916C and MGF4918D are super low noise InGaAs HEMTs manufactured by Mitsubishi Electric Corporation. FHR02X, FHX04X, FHX34X, FHX35X, FHX15X and FHR10X are the GaAs FET & HEMT Chips manufactured by Fujistu. MWTH4LN is the low noise Pseudomorphic GaAs HEMT manufactured by microwave technology. CFY66d08 is the K-Band GaAs Super Low Noise HEMT manufactured by infenion technologies.

Table 1. HEMT maximum ratings

Microwave Transistor (Chip HEMT)	V_{DS} (V)	V_{GS} (V)	I_D (mA)	P_D (mW)	F (GHz)	Gain (dB)
JS8901AS	4	-3	50	200	18	11
JS8902AS	4	-3	50	200	18	11
JS8905AS	4	-3	50	200	26	9
JS8910AS	3	-2.5	30	150	60	8
JS8911AS	4	-3	60	200	18	13
NE32400	4	-3	70	200	12	11
NE33200	4	-3	80	240	12	10.5
NE32484A	4	-3	70	165	12	11
NE32684A	4	-3	70	165	12	11.5
MGFC4416	-4	-4	60	50	12	12
MGF4916C	-4	-4	60	50	12	12
MGF4918D	-4	-4	60	50	12	11.5
FHR02X	3.5	-3	60	180	18	9
FHX04X	3.5	-3	60	180	12	10.5
FHX34X	3	-	36	290	12	10
FHX35X	3	-	32	290	12	10
FHX15X	2	-	36	180	12	13
FHR10X	2	-	28	180	18	9.2
MWTH4LN	6	-	66	280	26	11
CFY66D08	3.5	-3	60	200	20	11

Table 2. Performance parameters of HEMT

Microwave Transistor (Chip HEMT)	S_{11} (dB)	S_{12} (dB)	S_{21} (dB)	S22 (dB)	K	B
JS8901AS	-2.9	-14	-14	-4.4	3.6	0.9
JS8902AS	-4.6	-12	-12.6	-4.6	3.8	0.9
JS8905AS	-2.0	-12	-12.1	-4.8	2.1	1
JS8910AS	-1.5	-13	-13.9	-4.3	2.3	1
JS8911AS	-1.1	-18	-18.5	-4.1	4	1.1
NE32400	-1.2	-22	-22.6	-1.4	6	0.5
NE33200	-1.1	-20	-20.3	-1.9	3.9	0.6
NE32484A	-1.6	-9	-9.3	-1.4	1	0.3
NE32684A	-2.4	-6	-6.3	-1.8	1	0.2
MGFC4416	-1.6	-20	-20.5	-2	5.5	0.6
MGF4916C	-1.7	-13	-13.6	-1.4	1.5	0.4
MGF4918D	-1.2	-14	-14.1	-1.1	1.3	0.3
FHR02X	-1.2	-21	-21.3	-1.4	4.3	0.4
FHX04X	-1.3	-20	-20.7	-1.6	4.6	0.5
FHX34X	-1.6	-17	-17.5	-2.0	2.7	0.6
FHX35X	-1.7	-17	-17.0	-2.0	2.4	0.6
FHX15X	-0.9	-20	-20.1	-1.3	2.6	0.4
FHR10X	-1.0	-23	-23.7	-1.5	7.5	0.5
MWTH4LN	-2.5	-15	-15.7	-3.4	4.3	0.8
CFY66d08	-1.5	-9	-9.0	-1.8	1	0.4

Table 2 shows the comparison of 20 HEMTs with multiple parameters like input reflection coefficient (S_{11}), reverse transmission (S_{12}), forward transmission (S_{21}), output reflection coefficient (S_{22}), Rollete stability factor (K), and stability measurement (B). By simulating the corresponding HEMT at 30 GHz frequency and 10 dBm input power, all these values were attained. The optimal HEMT and accompanying parameter pair may be found in Table 2 and is as follows. The best combinations are "JS8902AS (S_{11}=–4.98 dB), NE32400 (S_{12}=–22.69 dB), NE32684A (S_{21}=–6.32 dB), FHR10X (K=7.5), and JS8911AS (B= 1.1)".

4. Basic Class E PA Comparative Analysis

Twenty HEMTs (listed in Table 2) are used in the design and simulation of the twenty basic class E power amplifiers depicted in Figure 2. Following simulation, a comparison of performance characteristics as shown in Table 3, was conducted in order to determine which HEMT would be most appropriate for applications involving millimeter wave frequency (30 GHz). The following is a list of the best HEMT and parameter pairs "JS8902AS (S22=-22.82dB), MWTH4HLN (S11=-5.0dB), JS8911AS (S12=-21.23dB), NE33200 (S21=6.18dB), JS8902AS (K=1.59), and JS8905AS (B=1.64)". Table 4 compares the performance metrics of twenty HEMT power amplifiers: DC power dissipation, output power (Pout), gain, Power Added Efficiency (PAE), and DE.

The following is a list of the finest HEMT pairs with matching parameters. "JS8901AS (PAE=39.31%), NE32484A (Gain=10.79dB) and JS89010AS (DE =55.38%)". Toshiba's T-shaped Gate, 0.2 µm JS8911AS, is the best-optimized transistor for 5G power amplifier at 30 GHz after a comparative analysis of 20 HEMT class E power amplifiers from Table 3 and Table 4. This is because of its high gain (9.85 dB), better PAE (31.87%), DE (33.55%), and good S parameters (S11= -0.72 dB, S12= -21.23 dB, S21= 5.62 dB, S22= -9.03 dB).

Table 3. Basic class E HEMTs power amplifier's S parameters & stability comparison

Microwave Transistor (Chip HEMT)	S_{11} (dB)	S_{12} (dB)	S_{21} (dB)	S_{22} (dB)	K	B
JS8901AS	-1.18	-16.90	2.37	-6.46	0.8	1.2
JS8902AS	-4.24	-17.72	4.37	-22.82	1.5	1.3
JS8905AS	-1.48	-15.83	3.47	-13.60	0.5	1.6
JS8910AS	-1.19	-17.14	0.07	-9.62	0.9	1.5
JS8911AS	-0.72	-21.23	5.62	-9.03	0.2	1.6
NE32400	-2.33	-17.98	4.24	-15.18	0.9	1.5
NE33200	-3.07	-16.41	6.18	-16.10	1	1.2
NE32484A	0.20	-11.85	2.61	-5.50	0	1.2
NE32684A	-1.36	-2.82	-15.21	-5.0	1.2	1.0
MGFC4416C	-3.37	-19.54	5.67	-14.63	1.4	1.3
MGF4916C	-1.21	-13.28	2.73	-4.88	-0.0	1.3
MGF4918D	-0.32	-13.18	2.98	-2.81	-0.3	1.0
FHR02X	-2.80	-18.11	2.33	-10.59	1.0	1.4
FHX04X	-2.83	-18.56	3.46	-10.19	1.1	1.3
FHX34X	-3.64	-17.83	3.71	-9.64	1.4	1.2
FHX35X	-3.36	-19.66	5.28	-11.54	1.3	1.3
FHX15X	-2.61	-19.16	5.64	-11.95	1.0	1.4
FHR10X	-2.71	-16.93	2.60	-11.57	1.0	1.4
MWTH4LN	-5.06	-16.36	3.36	-16.16	1.6	1.2
CFY66d08	-4.55	-15.85	0.16	-3.66	0.8	0.8

Table 4. Basic class E HEMTs power amplifiers performance comparison

Microwave Transistor (Chip HEMT)	P_{out} (mW)	P_{dc} (mW)	Gain (dB)	PAE (%)	DE (%)
JS8901AS	44	88	6.59	39.31	50.36
JS8902AS	29	89	3.73	18.72	32.45
JS8905AS	29	103	4.78	18.76	28.10
JS8910AS	30	54	4.69	36.60	55.38
JS8911AS	70	195	9.85	31.87	33.55
NE32400	40	89	7.07	35.77	44.50
NE33200	56	127	6.78	34.86	44.10
NE32484A	14	164	10.79	7.79	8.50
NE32684A	25	77	9.56	29.02	32.63
MGFC4416C	58	157	7.67	32.27	38.93
MGF4916C	15	87	7.54	14.23	17.27
MGF4918D	21	92	8.55	19.38	22.51
FHR02X	12	90	5.08	11.42	16.55
FHX04X	18	101	5.85	12.81	18.38
FHX34X	26	88	3.95	17.62	29.49
FHX35X	40	119	6.02	24.98	33.29
FHX15X	30	153	8.37	16.46	19.31
FHR10X	17	47	6.72	27.91	35.44
MWTH4LN	34	113	4.23	18.94	30.39
CFY66d08	9	100	1.52	2.65	8.93

5. Design and Simulation of Proposed Millimeter Wave Class E PA

It is quite difficult to fulfill the optimized requirements of strong linearity, high output power, less power reflection, greater stability, low power consumption, and high efficiency when designing a millimeter wave power amplifier for 5G applications [6]. Figure 4 illustrates the suggested class E power amplifier operating at 30 GHz and 6 mW of input power. It is designed using JS8911AS HEMT and incorporates a self-biased adjustable parallel RLC power control circuit at the common gate transistor. It is different from the traditional stacked power amplifier circuit [7, 8] but achieves all the optimized requirements of mm-wave PA.

In this circuit, two JS8901AS transistors are stacked with inductors. One common source stage transistor (M1) is excited with an RF input signal, and another common gate transistor (M2) is self-biased with a parallel RLC (R, L8 and C7) circuit. The impedance of a parallel RLC network can be varied with tunable capacitor C7, which controls the gate-to-source, gate-to-drain voltage and DC power. Here, the values of R, L8 and C7 are chosen to resonate at the operating frequency, i.e., 30 GHz, to obtain high impedance, which minimizes the DC power consumption and maximizes the PAE. Hence, the operating region of M2 and output power can be controlled based on the load requirements with the help of a tunable parallel RLC network. The cutoff and saturation state of M1 depend on the magnitude of the RF input signal. If it is in the cutoff region, then the Series Resonant Circuit (SLC1) starts charging through V_{DD} and M2. When the M1 goes into saturation region then the SLC1 starts discharging through the M1.

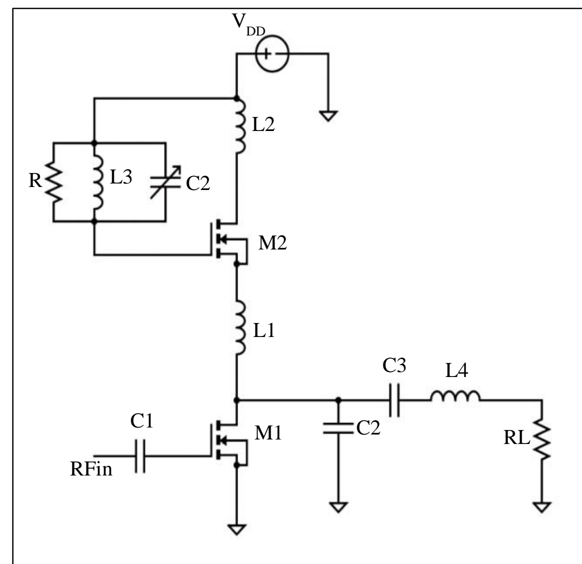

Fig. 4 Proposed self-biased tunable power controlled class-E power amplifier

This continuous charging and discharging of a series resonant circuit helps to get the power-amplified sinusoidal signal at the load. The proposed power amplifier output power is amplified to 152 mW with 6mW input power, and the gain, PAE, DE, S11, S12, S21, and S22 are 13.87 dB, 30.36%, 31.66%, 0.05 dB, -24.80 dB, 13.10 dB, -5.14 dB respectively.

Figure 5 shows the proposed class E power amplifier with JS8911AS equivalent circuit, where Cgd, Cgs, Rgs, Cds, Rds represent the intrinsic parasitics and Lg, Rg, Ld, Rd, Ls, Rs represent the extrinsic parasitic elements of HEMT. Figure 6 is the proposed single-stage stacked Class E power amplifier, which is designed and simulated using Keysight ADS. The same stacked power amplifier (PA1, PA2) is used to design the two-way Doherty power amplifier [9, 10] as shown in Figure 7 with Power Divider (PD), Power Combiner (PC) and 90 degree Phase Shifter (PS), to improve the gain and power added efficiency. Figure 8 shows the layout of the Doherty power amplifier.

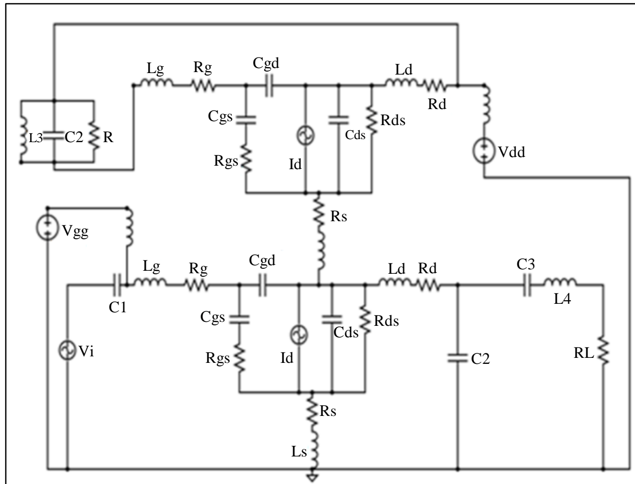

Fig. 5 Proposed power amplifier with small signal HEMT equivalent model

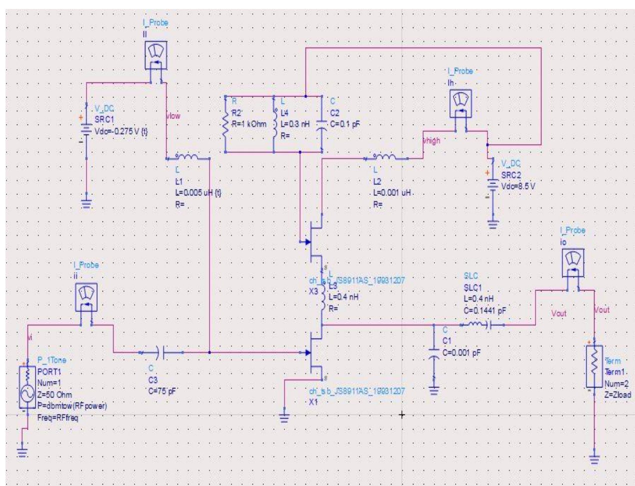

Fig. 6 Proposed single-stage stacked class E power amplifier designed using keysight ADS

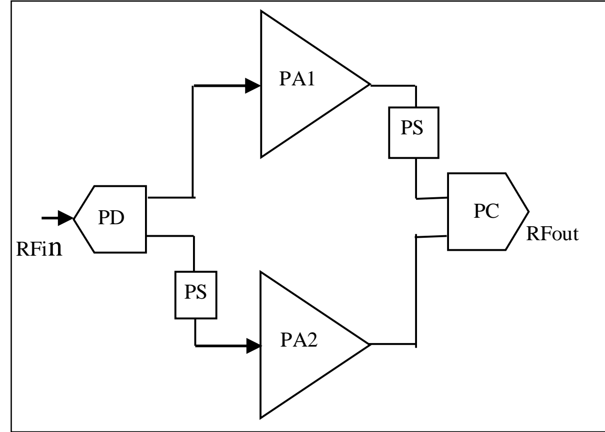

Fig. 7 Doherty power amplifier

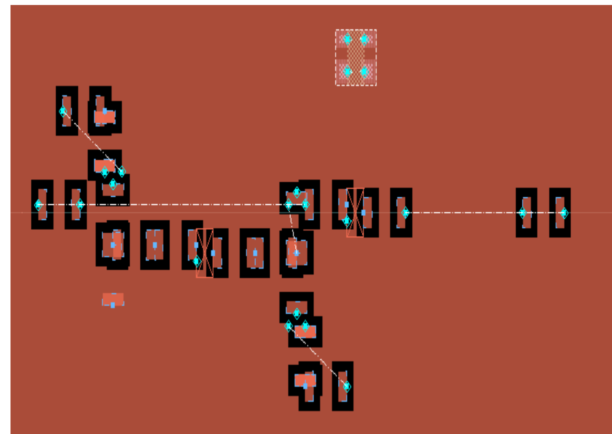

Fig. 8 Layout of millimeter two-way Doherty stacked class-E PA

6. Results and Discussion

Figure 9 (a) to (d) shows the output power, PAE, Gain, S12, and S21 parameters as 701 mW, 79.34 %, 20.85 dB, -20.21 dB, 17.69 dB, respectively.

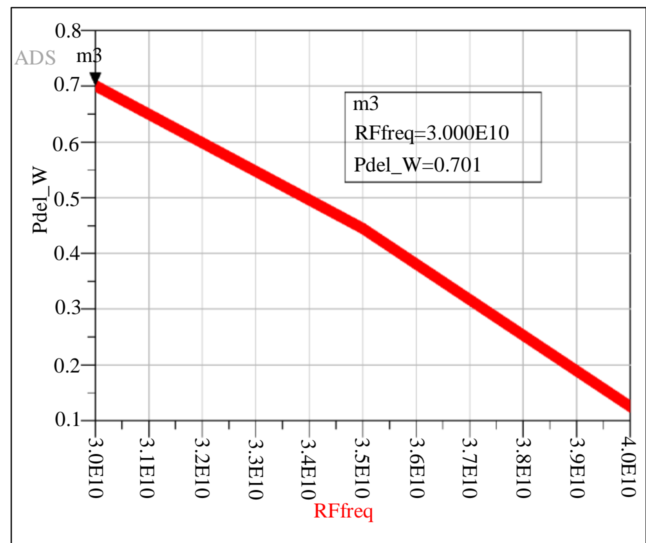

(a)

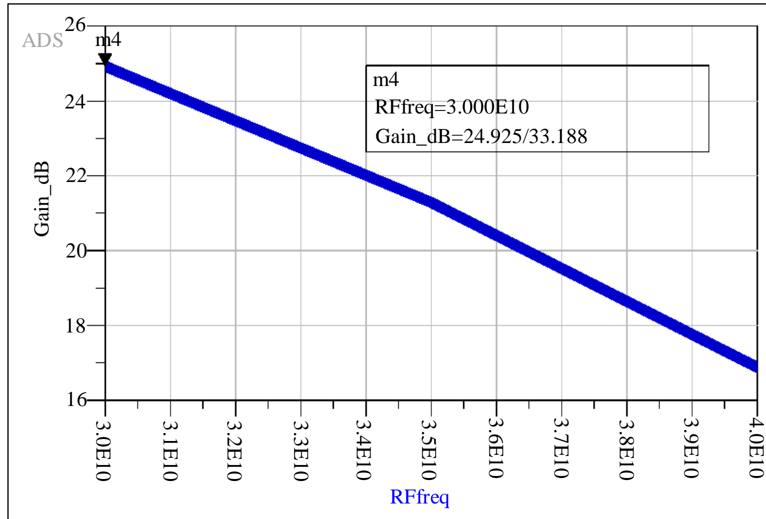

(b)

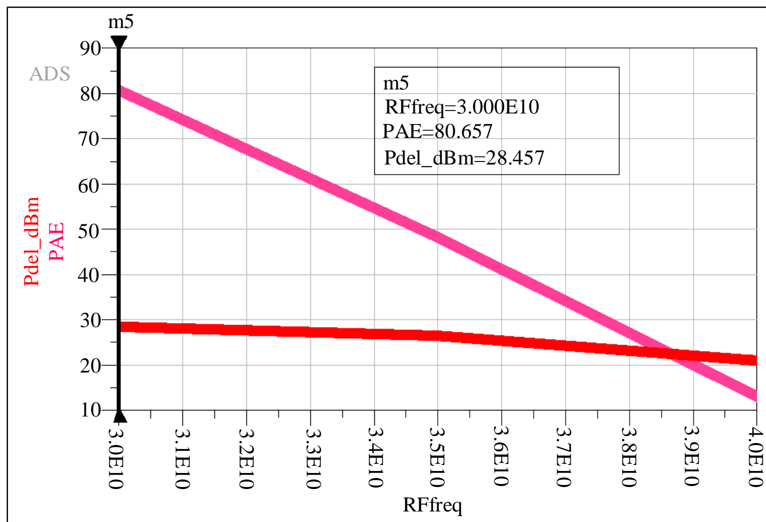

(c)

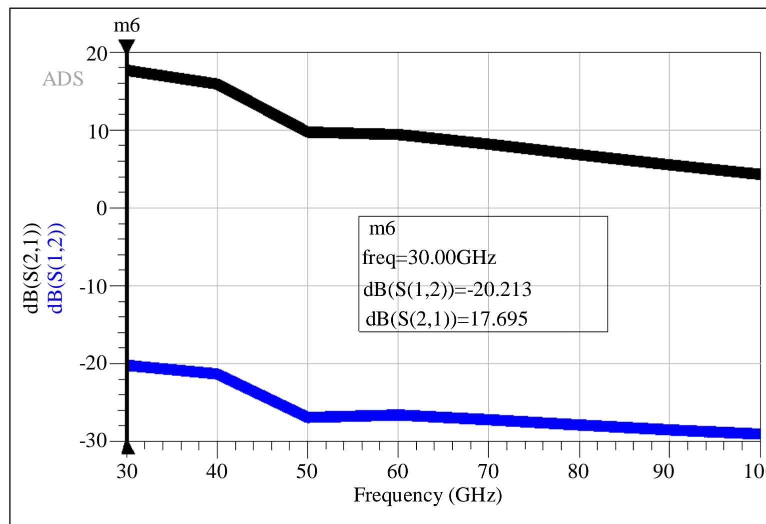

(d)

Fig. 9 30GHz Two-way Doherty stacked class E PA (a) Output power, (b) Gain, (c) PAE and output power (dBm), and (d) S parameters.

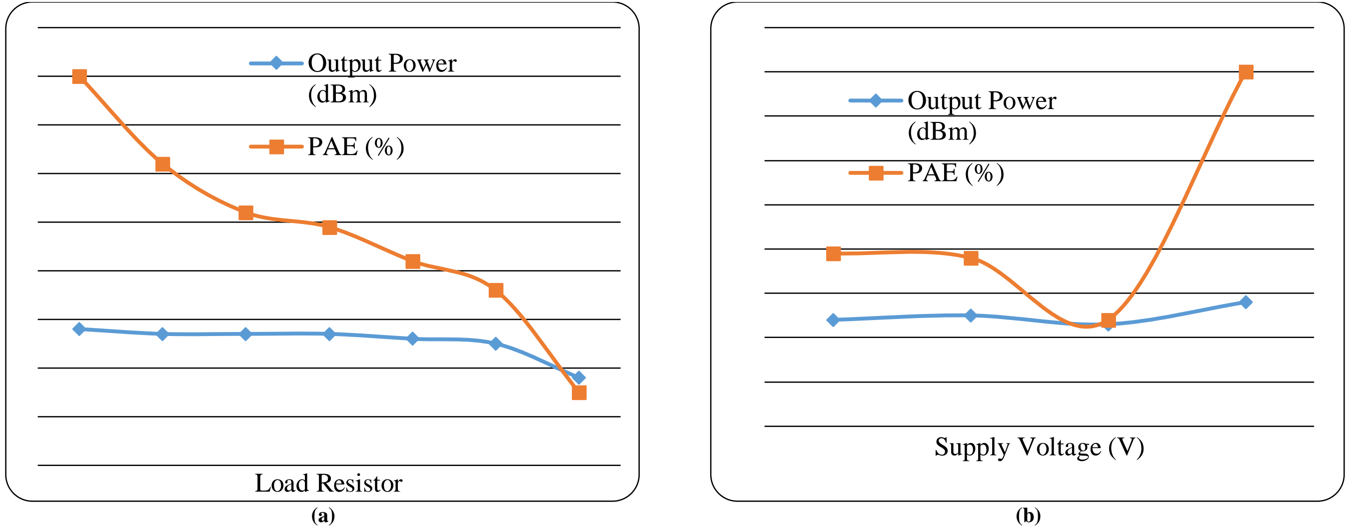

Fig. 10 Variation of output power and PAE with (a) Load resistor, and (b) Supply voltage.

Table 5. k-band Doherty PA performance comparison

Reference	Technology	Max Frequency (GHz)	Final Stage Topology	Output Power (dBm)	PAE (%)	Gain (dB)
[11]	0.1 μm GaN HEMT	27	Filter-Based Matching Networks	30.9	35.6	28.6
[12]	0.1 μm GaN HEMT	27	Filter-Based Matching Networks	30.3	36.9	24
[13]	150 nm GaAs pHEMT	25	Doherty	30.2	37	10
[14]	90 nm GaAs pHEMT	30.5	Doherty	30	40	-
[15]	0.15 μm GaAs pHEMT	30	Power combining	22	36.5	-
[16]	0.1 μm GaAs pHEMT	37	Doherty	28	33.2	15.6
[17]	90 nm GaAs pHEMT	39	Dual-band Matching Networks	23.8	51.7	20.3
[18]	45 nm SOI CMOS	40	load modulated balanced amplifier	25.1	27.9	-
[19]	0.25 μm GaAs pHEMT	16.5	Power combining	29.6	38.4	18.1
[20]	0.15 μm GaAs pHEMT	18	reconfigure bias choke	21.3	28	-
[21]	0.15 μm GaAs pHEMT	58	2-stage cascade	18.6	18.2	14.7
This Work	200 nm GaAs HEMT	30	Stacked, Doherty	28.46	80	24.9

Figure 10 (a) and (b) show the variation of output power in dBm and PAE in percentage with respect to Load Resistor and Supply Voltage, respectively. The proposed self-bias parallel RLC power control circuit is used to control the DC power and PAE of the power amplifier with the help of a variable capacitor (C2), as shown in Figure 11. Table 5 shows the comparison of cascode stacked Doherty power amplifier performance with previous work.

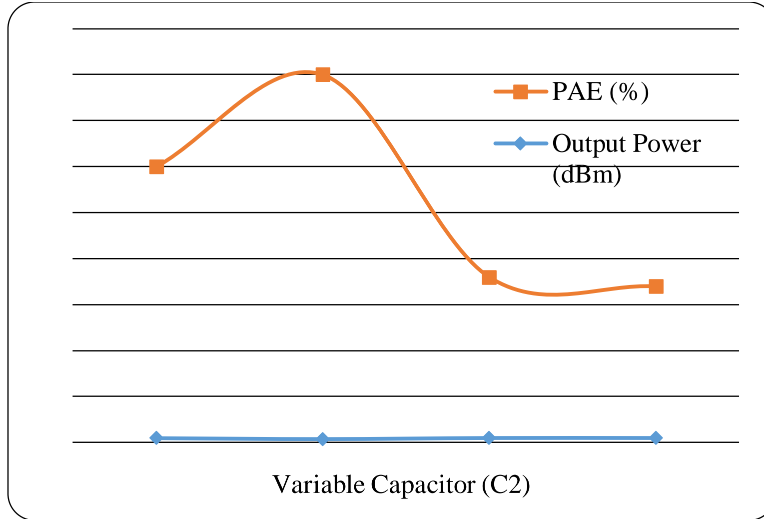

Fig. 11 Variation of output power and PAE with variable capacitor (C2)

7. Conclusion

To understand the performance of microwave/HEMT transistors at millimetre wave frequency 30 GHz, the twenty basic class-E power amplifiers are designed, and comparative analysis has been done to identify the better HEMT.

After comparative analysis, the T-shaped Gate, 0.2 µm GaAs HEMT, i.e. Toshiba's JS8911AS, is chosen due to its high gain and better stability. Later, the stacked and two-way Doherty power amplifiers are designed with a novel self-biased tunable parallel RLC power control circuit at 30 GHz radio frequency input signal and observed the well-improved gain (24.9 dB), output power (28.46 dBm), power added efficiency (80 %), forward (17.69 dB) and reverse (-20.21 dB) transmission coefficients.

Acknowledgments

The authors wish to thank the Central University of Karnataka, Kalaburagi for providing the necessary resources for the preparation of this manuscript.

References

[1] H.F. Cooke, "Microwave Transistors: Theory and Design," *Proceedings of the IEEE*, vol. 59, no. 8, pp. 1163-1181, 1971. [CrossRef] [Google Scholar] [Publisher Link]

[2] Nikhil Saxena, Pankaj Agarwal, and Sonal Soni, "Design and Analysis of Cascode Amplifier with Improved Gain," *Journal of Computational and Theoretical Nanoscience*, vol. 14, no. 11, pp. 5654-5656, 2017. [CrossRef] [Google Scholar] [Publisher Link]

[3] Hayg-Taniel Dabag et al., "Analysis and Design of Stacked-FET Millimeter-Wave Power Amplifiers," *IEEE Transactions on Microwave Theory and Techniques*, vol. 61, no. 4, pp. 1543-1556, 2013. [CrossRef] [Google Scholar] [Publisher Link]

[4] Richard Kubowicz, "*Class E Power Amplifier*," Thesis, University of Toronto, 2000. [Google Scholar] [Publisher Link]

[5] N.O. Sokal, and A.D. Sokal, "Class E-A New Class of High-Efficiency Tuned Single-Ended Switching Power Amplifiers," *IEEE Journal of Solid-State Circuits*, vol. 10, no. 3, pp. 168-176, 1975. [CrossRef] [Google Scholar] [Publisher Link]

[6] D.Y.C. Lie et al., "A Review of 5G Power Amplifier Design at cm-Wave and mm-Wave Frequencies," *Wireless Communications and Mobile Computing*, vol. 2018, pp. 1-16, 2018. [CrossRef] [Google Scholar] [Publisher Link]

[7] Peter Asbeck et al., "Stacked Si MOSFET Strategies for Microwave and Mm-Wave Power Amplifiers," *2014 IEEE 14th Topical Meeting on Silicon Monolithic Integrated Circuits in RF Systems*, Newport Beach, USA, pp. 13-15, 2014. [CrossRef] [Google Scholar] [Publisher Link]

[8] Rosendo Peña-Eguiluz et al., "Stacked Class-E Amplifier," *IEEE Transactions on Industrial Electronics*, vol. 67, no. 10, pp. 8292-8301, 2020. [CrossRef] [Google Scholar] [Publisher Link]

[9] Young Chan Choi et al., "Doherty Power Amplifier with Extended High-Efficiency Range Based on the Utilization of Multiple Output Power Back-Off Parameters," *IEEE Transactions on Microwave Theory and Techniques*, vol. 70, no. 4, pp. 2258-2270, 2022. [CrossRef] [Google Scholar] [Publisher Link]

[10] Debajit De et al., "Design and Analysis of Various Wilkinson Power Divider Networks for L Band Applications," *2016 3rd International Conference on Signal Processing and Integrated Networks (SPIN)*, Noida, India, pp. 67-72, 2016. [CrossRef] [Google Scholar] [Publisher Link]

[11] Lin Peng et al., "Design of an Efficient 24-30 GHz GaN MMIC Power Amplifier Using Filter-Based Matching Networks," *Electronics*, vol. 11, no. 13, pp. 1-18, 2022. [CrossRef] [Google Scholar] [Publisher Link]

[12] Lin Peng et al., "Design of Broadband High-Gain GaN MMIC Power Amplifier Based on Reactive/Resistive Matching and Feedback Technique," *IEICE Electronics Express*, vol. 18, no. 19, pp. 1-6, 2021. [CrossRef] [Google Scholar] [Publisher Link]

[13] Chiara Ramella et al., "Watt-Level 21–25-GHz Integrated Doherty Power Amplifier in GaAs Technology," *IEEE Microwave and Wireless Components Letters*, vol. 31, no. 5, pp. 505-508, 2021. [CrossRef] [Google Scholar] [Publisher Link]

[14] Heng Xie et al., "A Ka-Band Watt-Level High-Efficiency Doherty Amplifier MMIC in 90-nm GaAs Technology," *IEEE Microwave and Wireless Technology Letters*, vol. 33, no. 2, pp. 204-207, 2023. [CrossRef] [Google Scholar] [Publisher Link]

[15] Jiajin Li et al., "A mm-Wave Parallel-Combined Power Amplifier Supporting Balanced/Unbalanced Mode for 5G NR FR2 Applications," *IEEE Microwave and Wireless Technology Letters*, vol. 33, no. 5, pp. 543-546, 2023. [CrossRef] [Google Scholar] [Publisher Link]

[16] Zuojun Wang et al., "A 37-GHz Asymmetric Doherty Power Amplifier With 28-dBm P_{sat} and 32% Back-Off PAE in 0.1-µm GaAs Process," *IEEE Transactions on Microwave Theory and Techniques*, vol. 70, no. 2, pp. 1391-1400, 2022. [CrossRef] [Google Scholar] [Publisher Link]

[17] Heng Xie et al., "A High-Efficiency 28 GHz/39 GHz Dual-Band Power Amplifier MMIC for 5G Communication," *IEEE Microwave and Wireless Components Letters*, vol. 31, no. 11, pp. 1227-1230, 2021. [CrossRef] [Google Scholar] [Publisher Link]

[18] Lang Chen et al., "A 40-GHz Load Modulated Balanced Power Amplifier Using Unequal Power Splitter and Phase Compensation Network in 45-nm SOI CMOS," *IEEE Transactions on Circuits and Systems I: Regular Papers*, vol. 70, no. 8, pp. 3178-3186, 2023. [CrossRef] [Google Scholar] [Publisher Link]

[19] Chunshuang Xie et al., "An X/Ku Dual-Band Switchless Frequency Reconfigurable GaAs Power Amplifier," *IEEE Microwave and Wireless Components Letters*, vol. 32, no. 6, pp. 539-542, 2022. [CrossRef] [Google Scholar] [Publisher Link]

[20] Shijie Chen et al., "A 0.8-to-18 GHz Nonuniform Distributed PA Using Reconfigurable Bias Choke in 0.15 µm GaAs pHEMT," *IEEE Microwave and Wireless Technology Letters*, vol. 33, no. 9, pp. 1309-1312, 2023. [CrossRef] [Google Scholar] [Publisher Link]

[21] Yi-Fan Tsao, and Heng-Tung Hsu, "A 52-58 GHz Power Amplifier with 18.6-dBm Saturated Output Power for Space Applications," *IEEE Transactions on Circuits and Systems II: Express Briefs*, vol. 68, no. 6, pp. 1927-1931, 2021. [CrossRef] [Google Scholar] [Publisher Link]